Glycopolymer Decoration of Gold Nanoparticles Using a LbL Approach

Cyrille Boyer,* Antoine Bousquet, John Rondolo, Michael R. Whittaker, Martina H. Stenzel, and Thomas P. Davis*

Centre for Advanced Macromolecular Design (CAMD), School of Chemical Engineering, The University of New South Wales, Sydney NSW 2052, Australia

ABSTRACT: Two different copolymers, i.e., poly(*tert*-BuA-*co*-chloromethylstyrene) and poly(*tert*-BuA-*co*-HEA), were synthesized by reversible addition−fragmentation (RAFT) polymerization. A poly(*tert*-BuA-*co*-chloromethylstyrene) copolymer was subsequently modified by thioglucose using a thio−halogen click nucleophilic substitution reaction. A poly(*tert*-BuA-*co*-HEA) copolymer was subsequently modified by *p*-toluenesulfonyl chloride, followed by sugar functionalization (galactose) via a nucleophilic substitution reaction. The resultant glycopolymers were characterized by NMR, FTIR, and GPC analyses. Both glyco-modification procedures were shown to be highly efficient with yields close to 100%. After deprotection of the *tert*-butyl groups to form carboxylic acid functionality, the copolymers were assembled onto positively charged gold nanoparticle (GNPs) surfaces using a layer-by-layer (LbL) methodology to yield sugar-functional GNPs. The glycopolymer-coated nanoparticles were characterized by transmission electron microscopy (TEM), UV−vis spectroscopy, dynamic light scattering (DLS), zeta-potential, and X-ray photoelectron spectroscopy (XPS). Finally, the presence of accessible sugar moieties on the surface of the GNPs was confirmed by a binding assay with Con A.

Introduction

Hybrid organic/inorganic nanostructures are of great interest for application in numerous medical and nanotechnology fields.[1−6] Gold and iron oxide nanoparticles are two of the most promising materials for sensing,[7] imaging applications,[8,9] gene,[3,9] and drug[10−13] delivery as their intrinsic properties (magnetism for IONPs and plasmon resonance for gold) and their low toxicity favor in vivo medical applications. However, to maintain colloidal stability in aqueous media, the nanoparticles require modification by low or high molecular weight organic compounds. The utilization of polymers to coat inorganic nanoparticles can result in beneficial properties imparted to the resultant hybrid nanoparticles, including the provision of functional groups on the nanoparticle surfaces. In addition, a polymer layer can be used to encapsulate therapeutic agents.[1] Two different synthetic strategies are widely used to attach polymers: "grafting-from" or "-onto"[8,14−16] or a layer-by-layer (LbL) assembly approach.[17−24] These two alternative approaches yield differently surface structured nanoparticles, either a polymer brush structure (grafting) or a multilayered structure comprised of entangled polymers held together by (normally) electrostatic attraction or hydrogen bonding. Several previous publications have described the LbL approach to yield nanocapsules or microcapsules in detail[17,18,21,22,25−30] or for the synthesis of nanomaterials for MRI applications[31] and gene/drug delivery.[32−36] One drawback of the LbL approach is that the polymer design is often driven by the requirements of the self-assembly process and thus the inclusion of specific functional groups can be problematic, although in recent work Caruso's group has proposed the postfunctionalization of hybrid organic/inorganic nanoparticles obtained using a LbL approach exploiting click chemsitry (azide−alkyne)[37] or thiol−ene chemistry[38] to both cross-link the layered polymer chains and introduce functional groups (poly(ethylene oxide) segments). Two other examples were also recently reported by Decher et al. for the functionalization of gold nanoparticles using LbL methodology to attach a fluorescence label[39] or doxorubicin (model drugs).[36] The authors describe the use of GNPs/LbL nanoparticles for the transport and the delivery of doxorubicin in vitro.[36]

In the current paper, we propose an efficient route to glycopolymer-coated gold nanoparticles using the LbL strategy. Glycopolymers have attracted interest as oligosaccharides play roles in mediating interactions between ligands and cell surface receptors[40] and specific protein interactions[41−43] for targeting applications.[44] Recently, it was confirmed that synthetic glycopolymers can mimic the function of naturally occurring polysaccharides.[45] This has stimulated research into synthesizing well-defined glycopolymers by exploiting free radical polymerization and living radical polymerization, such as reversible addition−fragmentation (RAFT),[46−49] atom transfer polymerization (ATRP),[50−52] nitroxide-mediated polymerization (NMP),[53] and iodine transfer polymerization.[54] The synthesis of synthetic glycopolymers requires the design and synthesis of precursor sugar monomers. Glycomonomer synthesis can often be quite intricate, involving multiple steps and arduous purification procedures.[55] CAMD, in earlier work, has developed a library of glycopolymers made using RAFT polymerization.[56−63] An alternative synthetic approach to glycopolymers can involve postmodification of a preformed polymer with active sugar substrates, yielding functional glycopolymer macromolecules. Recently, this approach has been favored, using "click" chemistries,[64,65] e.g., Cu(I)-catalyzed azide−alkyne cycloaddition (CuAAC),[41,45] thiol−ene reactions,[66−68] *p*-fluoro-thiol/amine reactions,[69,70] or activated esters.[71,72]

In this paper, we describe two new approaches to the synthesis of glycopolymers using very efficient and versatile reactions. Subsequently, these glycopolymers were self-assembled on gold nanoparticles surfaces using a layer-by-layer methodology to yield functional nanomaterials. According to our knowledge, the introduction of sugar moieties to the surface of gold nanoparticles using LbL is a novel approach, although Narain et al.

*Corresponding authors. E-mail: cboyer@unsw.edu.au (C.B.); t.davis@unsw.edu.au (T.P.D.).

Scheme 1. Schematic Strategy Used for the Functionalization of Gold Nanoparticles (GNPs) Using Layer-by-Layer Methodology
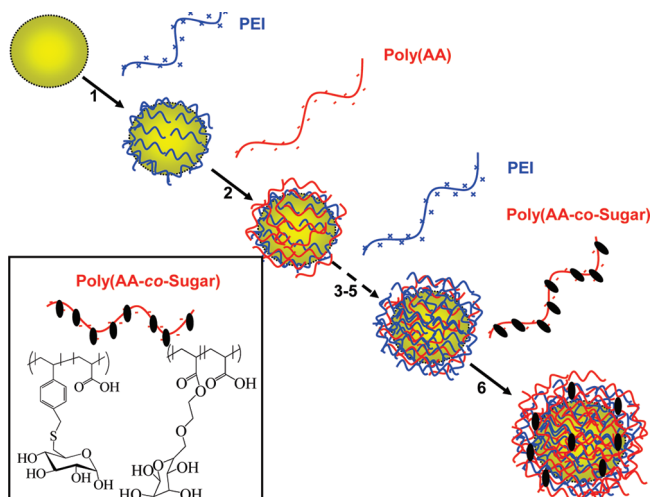
have proposed the decoration of gold nanoparticles by glyco-polymers using a grafting "onto" approach.[73−75] Finally, we demonstrated that GNPs modified with glycopolymers undergo specific interactions with proteins, such as lectin.

Experimental Part

1. Materials. 3-Benzylsulfanylthiocarbonylsulfanylpropionic acid (BSPA) was synthesized according to an established procedure.[76] *tert*-Butyl acrylate (*tert*-BA, Aldrich, 98%), vinyl-benzene chloride (chloromethylstyrene, CSt, Aldrich, 98%), and hydroxyethyl acrylate (HEA, Aldrich, 96%) were all purified on a column of basic alumina (Ajax Finechem) and stored at −19 °C. 2,2′-Azobis(isobutyronitrile) (AIBN, Dupont) was re-crystallized twice from methanol prior to use and then stored at 4 °C. 1,2:3,4-Di-*O*-isopropylidene-D-galactopyranose (Aldrich, 97%), sodium thioglucose (Aldrich, 97%), *p*-toluenesulfonyl chloride (Aldrich, >98%), pyridine (AJAX, 99%), sodium hydride (Aldrich, 60% dispersion in mineral oil), tetrahydrofuran anhydrous (THF, Sigma-Aldrich, 99.9%), hydrogenotetra-chloroaurate(III) hydrate (HAuCl$_4$, 99.9%, Aldrich), and triso-dium citrate dehydrate (99%, Aldrich) were used as received.

2. Polymer Syntheses. *Synthesis of Poly(acrylic acid): Poly(AA).* 3-(Benzylsulfanylthiocarbonylsulfanyl)propionic acid (**3**, BSPA) (50 mg, 1.84×10^{-4} mol) and t*ert*-butyl acrylate (1.28 g, 1.0×10^{-2} mol) were mixed with acetonitrile (10 mL). AIBN (5.6 mg, 3.6×10^{-5} mol) was then added to the solution. The solution was degassed with nitrogen for 30 min. After degassing, polymerization was initiated by heating at 70 °C for 6 h. The resulting poly(*tert*-butyl acrylic) was isolated by evaporating the solvent and mono-mer. The resultant solid was then dissolved in a minimal amount of acetone and further precipitated in a mixture of methanol and water (60/40). This purification process was repeated twice. The resulting solids (1 g) were then dissolved in dichloromethane (10 mL), and trifluoroacetic acid (TFA) (10 equiv by *tert*-butyl groups) was added to cleave the *tert*-butyl groups to yield carboxylic acid groups. The resulting solution was purified via dialysis and then freeze-dried. The product was characterized by ^{1}H NMR, GPC, and FTIR. ^{1}H NMR (300 MHz, CDCl$_3$, 25 °C, ppm) = 2.5−2.1 (1nH, C*H* of the main chain), 2−1 (2nH, C*H*$_2$ of the main chain). *n* is the degree of polymerization (DP*n*) of AA.

Synthesis of Poly(tert-butyl acrylic-co-chloromethylstyrene): Poly(TBA-co-CS) Copolymer. **3**, BSPA (50 mg, 1.84×10^{-4} mol), vinylbenzene chloride (0.16 g, 1.0×10^{-3} mol), *tert*-B-A (1.16 g, 9.0×10^{-3} mol), AIBN (5.6 mg, 3.6×10^{-5} mol) and acetonitrile (9 mL) were mixed. The solution was purged with nitrogen for 30 min before polymerization at 60 °C for 12 h. The resulting polymer was precipitated in a mixture of water and

methanol (10/90). Volatile compounds were then evaporated to yield a yellow solid. The copolymer was precipitated in a mixture of water/methanol (50/50 v/v %). The solid was dried in an oven at 40 °C under vacuum, and finally, the copolymer was characterized by GPC and ^{1}H NMR spectroscopy. ^{1}H NMR (300 MHz, CDCl$_3$, 25 °C, ppm) = 7.5−6.5 (5n_1H, C*H* of aromatic ring), 4.6 (2n_1H, −C*H*$_2$−Cl), 2.5−2.1 (1n_1H + 1n_2H, C*H* of the main chain), 2.0−1.0 (2n_1H + 2n_2H, C*H*$_2$ of the main chain), 1.4 (9n_2H, −C(C*H*$_3$)$_3$). n_1 and n_2 are the degrees of polymerization (DPn) of chloromethyl-styrene and *tert*-BuA, respectively.

Thiolated Sugar Modification of Poly(tert-BA-co-CSt). β-D-Sodium thioglucose (100 mg, 5.4×10^{-4} mol) was dissolved in a small amount of dimethyl sulfoxide (DMSO). In a separate vial, poly(*tert*-BA-*co*-CS) (300 mg, 2.0×10^{-4} mol of chloromethyl-styrene) was dissolved in a mixture of acetone/DMSO (50/50 v/v-%). Both solutions were mixed and purged for 10 min using nitrogen. Triethylamine (0.1 mL) was added to the solution, and the reaction occurred over 16 h. The reaction yielded a colorless solution of poly(*tert*-butyl acrylic coglucose). The polymer was precipitated several times (at least three times) in water (to eliminate any excess of sugar). The copolymer was characterized by GPC and by ^{1}H NMR spectroscopy. ^{1}H NMR (300 MHz, CDCl$_3$, 25 °C, ppm) = 7.5−6.5 (5n_1H, C*H* of aromatic ring), 5.6−5.4 (1n_1*H*, anomeric C*H* sugar), 4.7−3.5 (9n_1H, C*H* from sugar −C*H*$_2$SC*H*$_2$ sugar), 2.5−2.1 (1n_1H + 1n_2H, C*H* of the main chain), 2.0−1.0 (2n_1H + 2n_2H, C*H*$_2$ of the main chain), 1.4 (9n_2H, −C(C*H*$_3$)$_3$). n_1 and n_2 are the degrees of polymerization (DPn) of chloromethylstyrene and *tert*-BuA, respectively.

Conversion of Thioglucose-Modified Poly(tert-BA-co-CSt) to Thioglucose-Modified Poly(AA-co-CSt). Thioglucose-modified poly(*tert*-BA-*co*-CSt) (1 g) was dissolved in dichloromethane. Trifluoroacetic acid (6 g, 10 equiv of TFA by *tert*-butyl groups) was added to the solution and allowed to react for 3 days at room temperature. The polymer was precipitated twice in petroleum ether. The polymer was dialyzed against water (MWCO = 3500 Da) for 3 days. The solution was then freeze-dried and characterized by ^{1}H NMR. ^{1}H NMR (300 MHz, D$_2$O, 25 °C, ppm) = 11−10 (large peak, −COO*H*), 7.5−6.5 (5n_1H, C*H* of aromatic ring), 5.6−5.4 (1n_1*H*, anomeric C*H* sugar), 4.7−3.5 (9n_1H, C*H* from sugar −C*H*$_2$SC*H*$_2$ sugar), 2.5−2.1 (1n_1H + 1n_2H, C*H* of the main chain), 2.0−1.0 (2n_1H + 2n_2H, C*H*$_2$ of the main chain). n_1 and n_2 are the degrees of polymerization (DPn) of chloromethylstyrene and AA, respectively.

Synthesis of Poly(tert-BA-co-HEA). In a typical experiment, *tert*-BA (1.16 g, 9.0×10^{-3} mol) and HEA (0.115 g, 1.0×10^{-3} mol) were dissolved in toluene (at [M]$_0$ = 3 mol L^{-1}) in a Schlenk tube. AIBN (5.6 mg, 3.6×10^{-5} mol) as initiator and BSPA (50 mg, 1.84×10^{-4} mol) as RAFT agent were added to the solution. The reaction mixture was sealed and deoxygenated by three freeze−evacuate−thaw cycles. Finally, the polymeri-zation was performed with stirring under a nitrogen atmosphere at 70 °C. At the end of the polymerization, toluene was removed under reduced pressure, and the polymer/monomer solution was precipitated three times in a methanol/water (1/1) mixture to remove remaining monomer. The yellow paste P(tBA-*co*-HEA) obtained was freeze-dried to remove any water traces followed by GPC and ^{1}H NMR analyses. ^{1}H NMR (300 MHz, CDCl$_3$, 25 °C, ppm) = 4.4−4.0 (4n_1H, COOC*H*$_2$CH$_2$OH), 3.9−3.6 (4n_1H, COOCH$_2$C*H*$_2$OH), 2.4−2.1 (1n_1H + 1n_2H, C*H* of the main chain), 2−1 (2n_1H + 11n_2H, C*H*$_2$ of the main chain + COOC(C*H*$_3$)$_3$). n_1 and n_2 are the degrees of polymer-ization (DPn) of HEA and *t*BA, respectively. An additional signal at 4.9−4.8 ppm (1n_1H, COOCH$_2$CH$_2$O*H*) was observed in acetone.

Synthesis of Poly(tert-BA-co-HEATS). Poly(*tert*-BA-*co*-HEA) (2 g, 1 equiv) and *p*-toluenesulfonyl chloride (pTSCl, 1.26 g, 30 equiv) were dissolved in pyridine (8 mL). After complete dissolution of polymer, the mixture was allowed to stir at ambient temperature for 14 h. The mixture was subsequently dialyzed against MeOH/water (1/1) to remove unreacted pTSCl

and pyridine. After rotary evaporation and freeze-drying, the modified polymer was characterized by GPC and ^{1}H NMR. ^{1}H NMR (300 MHz, acetone-d_6, 25 °C, ppm) = 7.9–7.7 ($2n_1$H, $O_3SCCH_2CH_2CCH_3$), 7.5–7.3 ($2n_1$H, $O_3SCCH_2CH_2CCH_3$), 4.4–4.1 ($4n_1$H, $COOCH_2CH_2O_3S$), 2.5–2.1 ($4n_1$H + $1n_2$H, CH of the main chain + $O_3SCCH_2CH_2CCH_3$), 2–1 ($2n_1$H + $11n_2$H, CH_2 of the main chain + $COOC(CH_3)_3$). n_1 and n_2 are the degrees of polymerization (DPn) of HEATS and *tert*-BA, respectively.

Synthesis of the Poly(tert-BA-co-HEA/Galactopyranose). In a typical experiment, sodium hydride (NaH 60% in oil, 260 mg, 30 equiv) was dissolved in dry THF (2 mL) under a nitrogen atmosphere before the reaction vessel was placed in a glovebox. A THF (4 mL) solution of 1,2,3,4-di-O-isopropylidene-D-galactopyranose (1.73 g, 30 equiv) was then added dropwise to the mixture. Finally, a THF (5 mL) solution of poly(*tert*-BA-*co*-HEATS) (2 g, 1 equiv) was introduced into the mixture. The flask was sealed with a septum, removed from the glovebox, and allowed to stir for 14 h at ambient temperature. Aqueous ammonium chloride solution (10 mL, $c = 1$ mol L^{-1}) was then added in order to destroy any residual sodium hydride, followed by a dialysis against MeOH/water (1/1). After removal of MeOH by rotary evaporation and water by freeze-drying, the polymer was characterized by GPC and by ^{1}H NMR spectroscopy. **Warning**: *this reaction creates H_2 (gas) and may induce an increase in pressure.* ^{1}H NMR (300 MHz, CDCl₃, 25 °C, ppm) = 5.6–5.4 ($1n_1$H, anomeric CH sugar), 4.7–3.8 ($6n_1$H, CH from sugar + $COOCH_2CH_2OCH_2$), 3.6–3.4 ($4n1$H, $COOCH_2CH_2OCH_2$), 2.5–2.1 ($1n_1$H + $1n_2$H, CH of the main chain), 2–1 ($14n_1$H + $11n_2$H, CH_2 of the main chain + CH_3 of the protected sugar + $COOC(CH_3)_3$). n_1 and n_2 are the degrees of polymerization (DPn) of HEAGalactopyranose and *tert*-BA, respectively.

Deprotection of the Poly(tert-BA-co-HEA/Galactopyranose). P(*tert*-BA-*co*-HEA/galactopyranose) was diluted in dichloromethane. Trifluoroacetic acid (10 equiv/monomer unit) was then added to the solution. The mixture was allowed to stir for 3 days at room temperature. The white solid precipitate was diluted in water, dialyzed against water with a membrane cutoff of 3500 Da, and finally freeze-dried. The statistical copolymer P(AA-*r*-HEA/galactose) was characterized by ^{1}H NMR. ^{1}H NMR (300 MHz, D₂O, 25 °C, ppm) = 4.6–4.5 ($1n_1$H, anomeric CH sugar), 4.4–3.4 ($8n_1$H, CH from sugar + $COOCH_2CH_2$-OCH_2), 2.5–2.1 ($1n_1$H + $1n_2$H, CH of the main chain), 2–1 ($2n_1$H + $2n_2$H, CH_2 of the main chain). n_1 and n_2 are the degrees of polymerization (DPn) of HEAGalactose and AA, respectively.

3. Functionalization of Gold Nanoparticles by LBL. *Synthesis of Gold Nanoparticles (GNPs).* Citrate-stabilized gold nanoparticles (20 nm) were prepared using published procedures.[77] Briefly, all glassware was first washed with an aqua-regia solution (25 vol % nitric acid and 75 vol % of concentrated hydrochloric acid), then rinsed with Milli-Q water several times, and dried. Milli-Q water (100 mL) and 1% solution trisodium citrate dehydrate (5 mL, 1.053 g of trisodium citrate) were mixed. The solution was heated up to boiling point with vigorous stirring, and then hydrogenotetrachloroaurate(III) hydrate stock solution (0.01 M) (2.54 mL) was introduced rapidly using a syringe. The solution was boiled for a further 30 min with vigorous stirring. A progressive change of color was observed from yellow to winered. The solution was cooled and stored in a fridge at 5 °C until required. The particles were characterized by TEM and DLS analyses. TEM pictures indicated well-dispersed gold nanoparticles with a diameter size around 20 nm, in accord with DLS results.

Layer-by-Layer Formation. All glassware was washed with aqua regia before use.

First Layer: Polyethylenimine (PEI) (Cationic). Commercially available PEI (500 mg) was dissolved in water (5 mL) and gently stirred for 30 min. A previously prepared citrate-capped gold nanoparticle solution (50 mL, 1 mg/mL) was added dropwise to the polymer solution using a glass pipet. The solution maintained a deep red color with very little color change. The solution

was left stirring for 2 h. GNPs were purified via high-speed centrifugation at 15 000 rpm for 40 min and redispersed in water (the process was repeated three times). The particles were characterized via UV–vis spectroscopy, TEM, DLS, and zeta-potential analysis.

Second Layer: PAA (Anionic). PAA polymer (100 mg) was dissolved in water (1 mL) in the presence of sodium carbonate to dissolve PAA. The PEI-coated GNP solution was carefully added to the polymer solution using a glass pipet. The solution maintained a red color. The solution was allowed to stir for 2 h. A slight shift from red to pink was noted. GNPs were purified using a similar process to that described above for the first layer. GNPs were characterized by DLS, XPS, TEM, zeta-potential, and UV–vis spectroscopy The process was repeated several times to yield a polymer multilayer encapsulating the GNPs.

A similar assembly process was used for poly(*tert*-AA-*co*-HEA/galatopyranose) copolymers.

4. Interactions of GNPs with Concanavalin A (Con A). 100 μL of Con A solution (1 mg/mL) was introduced to GNPs modified sugar moieties (1 mg/mL). The solution was gently shaken for 5 min using a pipet. After 15 min, the solution was analyzed by UV–vis and DLS. The solution was kept in the fridge for 1 night to allow the formation of a precipitate (in the case of GNPs modified P(AA-*co*-glucose)). 100 mg of glucose was added, and the solution was gently shaken. GNPs were analyzed by DLS and UV–vis.

A similar experiment was carried out for non-glycofunctional GNPs, i.e., GNPs/PEI/.../PAA.

5. Analyses. *Gel Permeation Chromatography (GPC) Measurements.* THF GPC was performed on a Shimadzu modular system, comprised of an autoinjector and a Polymer Laboratories 5.0 μm bead size guard column (50 × 7.5 mm), followed by three linear PL column and a differential refractive index detector using THF as the eluent at 40 °C with a flow rate of 1 mL min^{-1}. The GPC system was calibrated using linear polystyrene standards. DMAc GPC analyses of the polymers were performed in N,N-dimethylacetamide [DMAc; 0.03% w/v LiBr, 0.05% 2, 6-dibutyl-4-methylphenol (BHT)] at 50 °C (flow rate = 1 mL/min) using a Shimadzu modular system comprised of an SIL-10AD autoinjector and a PL 5.0 mm bead-size guard column (50 × 7.8 mm) followed by four linear PL (Styragel) columns (10^5, 10^4, 10^3, and 500 Å) and an RID-10A differential refractive index detector. Calibration was achieved with commercial polystyrene standards ranging from 500 to 10^6 g/mol.

Nuclear Magnetic Resonance (NMR). Structures of the synthesized compounds were analyzed by ^{1}H NMR spectroscopy using a Bruker DPX 300 spectrometer at 300 MHz for hydrogen nuclei and 75 MHz for carbon nuclei.

UV–vis Spectroscopy. UV–vis spectra were recorded using a CARY 300 spectrophotometer (Bruker) equipped with a temperature controller.

Zeta Potential and Dynamic Light Scattering. Dynamic light scattering studies of the GNPs at 1 mg/mL in aqueous media were conducted using a Malvern Zetasizer Nano Series running DTS software and operating a 4 mW He–Ne laser at 633 nm. Analyses were performed at an angle of 90°. GNP (or GNP/polymer) solutions were prepared in distilled water with a GNP concentration of 1 mg/mL. The solution was filtered through Millipore nylon filters (pore size 0.45 μm) to eliminate dust and large contaminants. The size measurements were carried out in quartz cuvettes at 25 °C, and the temperature was allowed to equilibrate for 5 min. The number-average hydrodynamic particle size and polydispersity index were determined by DLS based on an average of five measurements. The polydispersity index (PDI) was used to describe the width of the particle size distribution and was calculated from a cumulants analysis of the DLS measured intensity autocorrelation function and is related to the standard deviation of the hypothetical Gaussian distribution (i.e., PDI = σ^2/Z_D^2, where σ is the standard deviation and Z_D is the Z average mean size).

Transmission Electron Microscopy. The sizes and morphologies of the nanoparticles were observed using a transmission

electron microscopy JEOL1400 TEM at an accelerating voltage of 100 kV. The particles were dispersed in water (1 mg/mL) and deposited onto 200 mesh, holey film, copper grid (ProSciTech) and allowed to air-dry at room temperature.

X-ray Photoelectron Spectrometer (XPS). A Kratos Axis ULTRA XPS incorporating a 165 mm hemispherical electron energy analyzer was used. The incident radiation was monochromatic A1 X-rays (1486.6 eV) at 225 W (15 kV, 15 ma). Survey (wide) scans were taken at analyzer pass energy of 160 eV and multiplex (narrow) higher resolution scans at 20 eV. Survey scans were carried out over 1200−0 eV binding energy range with 1.0 eV steps and a dwell time of 100 ms. Narrow higher resolution scans were run with 0.2 eV steps and 250 ms dwell time. Base pressure in the analysis chamber was 1.0×10^{-9} Torr and during sample analysis 1.0×10^{-8} Torr. The data were analyzed by XPS peak 4.1.

Results and Discussion

Two different approaches were applied to decorate gold nanoparticles with glycopolymers using a layer-by-layer methodology. These two pathways used copolymer structures containing either chloromethylstyrene or hydroxylethyl acrylate together with *tert*-butyl acrylate which were prepared by RAFT polymerization. Both copolymer structures were then modified to incorporate glycopolymer functionality (Scheme 2).

1. Synthesis of Copoly(*tert*-BuA-*co*-chloromethylstyrene). The synthesis of copoly(*tert*-BuA-*co*-chloromethylstyrene) was achieved with RAFT polymerization, using BSPA as a RAFT agent and AIBN as a radical initiator. The theoretical

Scheme 2. Chemical Modification of Poly(*tert*-BuA-*co*-chloromethylstyrene) and Poly(*tert*-BuA-*co*-HEA) Copolymers by Sugar Compounds

A

1) TEA/ thio-sugar

B

1) TsCl (5eq) in Pyridine
2) Galactopyranose (2eq), NaH (2eq) in dry THF
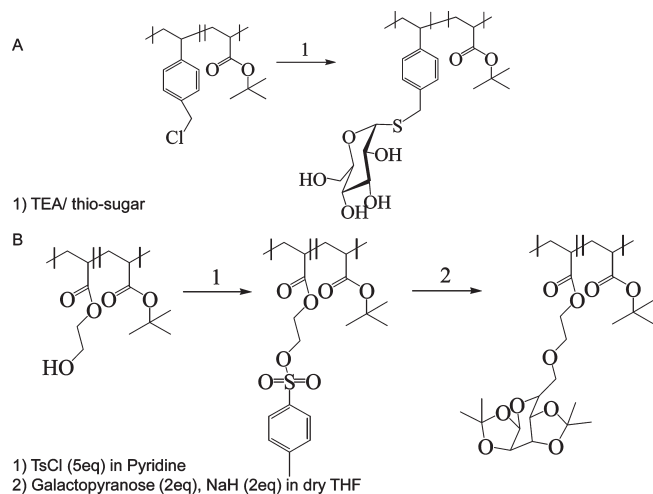
and experimental molecular weights (calculated by SEC and NMR) were consistent with a living copolymerization mechanism (Table 1). In addition, a narrow PDI was obtained at the end of the polymerization (PDI < 1.15). ^{1}H NMR analysis confirmed the presence of RAFT end-groups by a signal at 3.6 ppm attributed to $-S-CH_2$. The successful incorporation of chloromethylstyrene in the copolymers was also confirmed by the presence of aromatic signals (from 6.6 to 7.5 ppm) and the CH_2Cl signal at 4.6 ppm (see Figure 1A). The copolymer composition was close to the starting monomer feed composition, as calculated by ^{1}H NMR following the equation: chloromethylstyrene composition = $[I^{4.6\,ppm}]/[I^{2.0-1.0\,ppm}/(12 + (3 \times I^{4.6\,ppm})]$, with $I^{2.0-1.0\,ppm}$ and $I^{4.6\,ppm}$ are the integrals attributed to CH, CH$_2$, and C(CH$_3$)$_3$ signals and CH$_2$Cl, respectively.
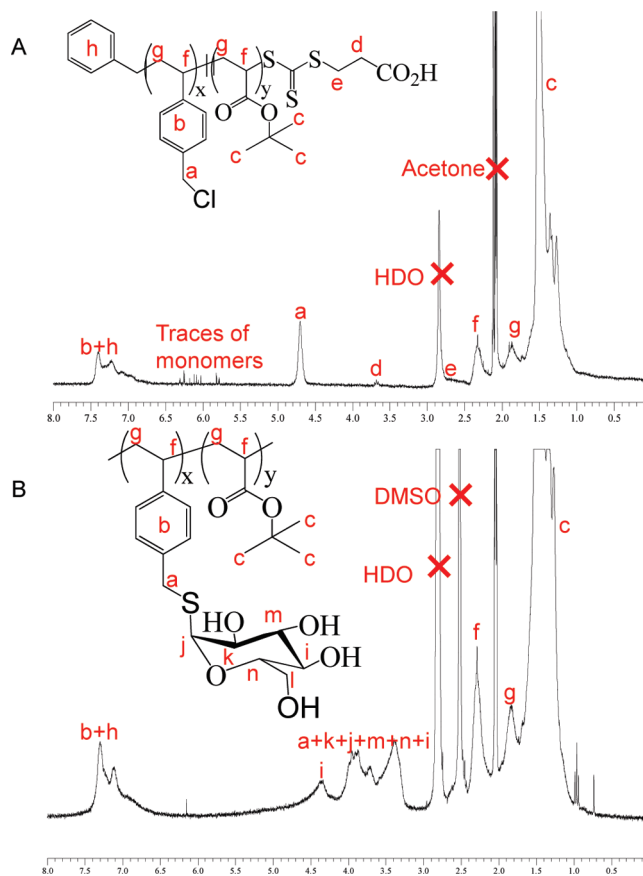
Figure 1. ^{1}H NMR spectra of (A) poly(*tert*-BuA-*co*-chloromethylstyrene) copolymers recorded in acetone-d_6 and copolymers modified after chloro-halogen click reaction recorded in DMSO-d_6.

Table 1. Characteristics of the Copolymers Synthesized for This Study[a]

copolymers	initial feed molar ratio (mol %)		composition in the copolymer (mol %)		average α^{M}	M_n^{theo} (g/mol)	M_n^{GPC} (g/mol)	PDI	M_n^{NMR} (g/mol)
	tert-BuA	mono[2]	*tert*-BuA	mono[2]					
poly(*tert*-BuA-*co*-chlorostyrene)	90	10	88	12	80	11 000	10 000	1.12	11 500
poly(*tert*-BuA-*co*-HEA)	90	10	90	10	95	12 500	11 000	1.14	12 000

[a] Composition of the copolymer and α^{M} calculated by ^{1}H NMR spectroscopy; Mono[2] corresponds to HEA or chloromethylstyrene; M_n^{theo} calculated by the following equation: $M_n^{theo} = \sum([Mi]_0/[RAFT]_0 \times MW^{Monomer,i}) \times \alpha^M + MW^{RAFT}$, where $[M]_0$, $[RAFT]_0$, $MW^{Monomer}$, α^M, and MW^{RAFT} correspond to initial monomer concentration with i is *tert*-BuA or HEA or chlorostyrene, initial RAFT agent concentration, molar mass of monomer, global monomer conversion, molar mass of RAFT agent, respectively; M_n^{GPC} determined by THF GPC using PSt calibration; M_n^{NMR} calculated by the following equations: in the case of poly(*tert*-BuA-*co*-chlorostyrene): $M_n^{NMR} = [I^{4.6\,ppm}/I^{3.6\,ppm}] \times MW^{Chlorostyrene} + [(I^{1.0-2.0\,ppm}/11)/(I^{3.6\,ppm}/2)] \times MW^{tert-BuA} + MW^{RAFT}$, with I^i are the integrals of peak at i ppm, $MW^{Chlorostyrene}$ and $MW^{tert-BA}$ correspond to molar mass of chlorostyrene and *tert*-BuA, respectively; in the case of poly(*tert*-BuA-*co*-HEA): $M_n^{NMR} = [I^{4.2\,ppm}/I^{3.6\,ppm}] \times MW^{HEA} + [(I^{1.0-2.0\,ppm}/11)/(I^{3.6\,ppm}/2)] \times MW^{tert-BA} + MW^{RAFT}$, with I^i are the integrals of peak at i ppm, MW^{HEA} and $MW^{tert-BA}$ correspond to molar mass of HEA and *tert*-BuA, respectively.
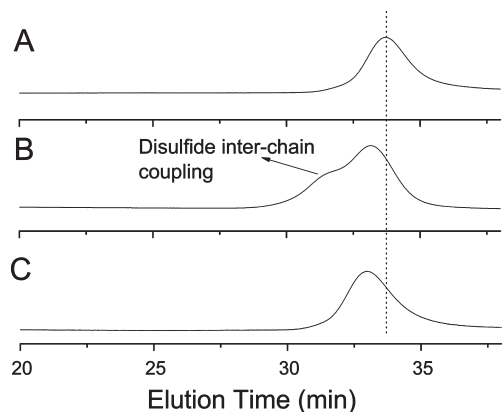
Figure 2. SEC traces of copolymers at different stages: (A) poly-(*tert*-BuA-*co*-chloromethylstyrene) copolymers before and (B) after modification with thio-glucose and (C) thio-glucose-modified poly-(*tert*-BuA-*co*- chloromethylstyrene) copolymers in the presence of dimethylphenylphosphine.

Figure 3. ATR-FTIR spectra of copolymers at different stages: (A) poly(*tert*-BuA-*co*-chloromethylstyrene) copolymers; (B) sodium thio-glucose spectra; (C) thio-glucose modified poly(*tert*-BuA-*co*-chloromethylstyrene) copolymers; (D) thio-glucose-modified poly-(AA-*co*-chloromethylstyrene) copolymers after deprotection of *tert*-butyl group by TFA treatment.

A thio-sugar, β-D-sodium thioglucose, was "clicked" onto the copolymer backbone via a "thio-halogen click" nucleophilic substitution reaction. Recently, the "thio-bromo" click reaction has been successfully employed[78,79] to functionalize polymers and to synthesize dendrimers or hyperbranched polymers. In the present work a "thio-chloro nucleophilic reaction" was employed. The reaction was performed with a [chloro]/[thio-sugar] molar ratio of 1.0/2.5 at room temperature for 16 h in mixed solvent: DMSO/acetone (50/50 v/v %) in the presence of triethylamine as catalyst. After purification by precipitation in water (to remove the thio-sugar), the polymers were dried to yield a white powder. A color change from yellow to colorless was observed consistent with the degradation of RAFT end-groups, in accord with an absence of any signal at 305 nm as measured by UV−vis spectra. The presence of free thiol in a solution of RAFT polymers can induce degradation, as reported by Harrison.[80] A significant change was observed in the ^{1}H NMR spectra after the copolymers were modified with sugar. First, the signal of −CH$_2$Cl at 4.6−4.7 ppm disappeared, while new and complex signals at 3.5−4.5 ppm appeared, attributable to sugar functionality. The reaction yield was estimated to be fully quantitative as the −CH$_2$Cl peak (4.6 ppm) completely disappeared. Moreover, each unit styrene was modified by one unit sugar, as calculated by the ratio of the integrals from the sugar and phenyl groups (yield = [∫3.5−4.5 ppm/11]/[∫6.5−7.5 ppm/5]). THF SEC traces show a slight shift from high retention time to low retention time, and a shoulder at low retention times (high molecular weight) was also observed (Figure 2). The high molecular weight shoulder can be attributed to the formation of disulfide interchain coupling caused by oxidation of the free thiol end-groups.[81,82] The degradation of RAFT end-groups (as previously noted by the absence of any absorption at 305 nm (C=S group) and by a color change from yellow to colorless) results in the formation of free thiol groups,[83] as confirmed by an Ellman's assay.[84,85] The presence of free thiol yields an absorption at 405 nm detectable by UV−vis spectroscopy (data not shown). In the presence of a reducing agent, such as dimethylphenylphosphine, the disulfide coupling product could be removed (Figure 2C).

Finally, the *tert*-butyl groups were cleaved to yield carboxylic acid groups using trifluoroacetic acid (TFA). The successful modification of the polymer was indicated by a s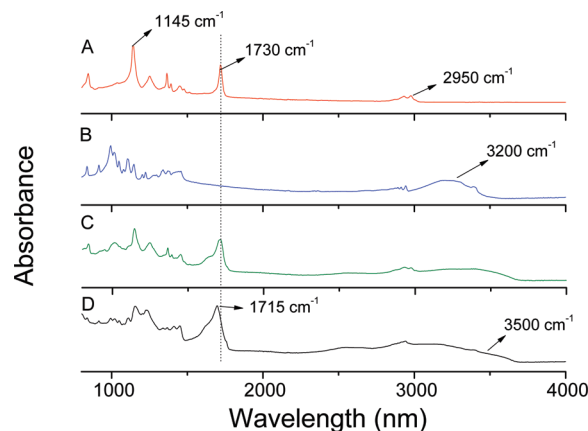ignificant change in solubility of the copolymer (the copolymer becomes water-soluble). FTIR analysis confirmed the presence of carboxylic acid groups (large absorption band from 3000 to 3500 cm^{-1}) and the disappearance of ester groups (absorption band at 1730 cm^{-1}). A new signal at 1715 cm^{-1} appears characteristic of carbonyl from the carboxylic acid group (Figure 3). In addition, the absence of a ^{1}H NMR signal at 1.4 ppm (*tert*-butyl groups) confirmed the success of the deprotection step.

2. Copolymerization of HEA and *tert*-Butyl Acrylate and Subsequent Functionalization by Galactose. In a second approach, we copolymerized hydroxyethyl acrylate (HEA) and *tert*-butyl acrylate using RAFT polymerization. Monomer consumption was monitored by ^{1}H NMR spectroscopy (Figures S1−S4 in the Supporting Information). The simultaneous consumption of both monomers was observed resulting in the synthesis of a statistical copolymer. After purification by precipitation, the copolymer was analyzed by ^{1}H NMR, confirming that the initial feed composition and copolymer composition were very similar (see Table 1 and Figure 4).

The hydroxyl end-groups were then modified by reaction with *p*-toluenesulfonyl chloride at room temperature in the presence of pyridine as catalyst. The reaction proved to be fully quantitative, as the hydroxyl signal (at 3.7 ppm) disappeared there was the concomitant appearance of the aromatic signal from the toluene group at 7.3 and 7.8 ppm. The *p*-toluene sulfonyl activates the hydroxyl group toward nucleophilic substitution. The pyridine catalyst also simultaneously cleaves the RAFT end-groups by aminolysis to yield thiol end-groups. The copolymer chains were subsequently modified with galactose in the presence of NaH (strong base) under anhydrous conditions. The sodium hydride (NaH) deprotonates alcohol forming alcoholate anions, able to react via nucleophilic substitution with the tosyl groups on the copolymer (see Scheme 2). During this reaction, the characteristic yellow color disappeared to yield a colorless solution. This loss of color corresponds to the degradation of the RAFT end-group. UV−vis spectroscopy confirms the lost of the characteristic C=S bond at 305 nm. After purification by precipitation, the copolymer was analyzed by ^{1}H NMR and GPC analyses. New NMR signals centered at 4.2, 4.6, and 5.5 ppm could be attributed to galactose functionality, while signals from the aromatic groups at 7.5 and 7.8 ppm disappeared. GPC analyses indicate a slight shift in the molecular weight distribution to lower
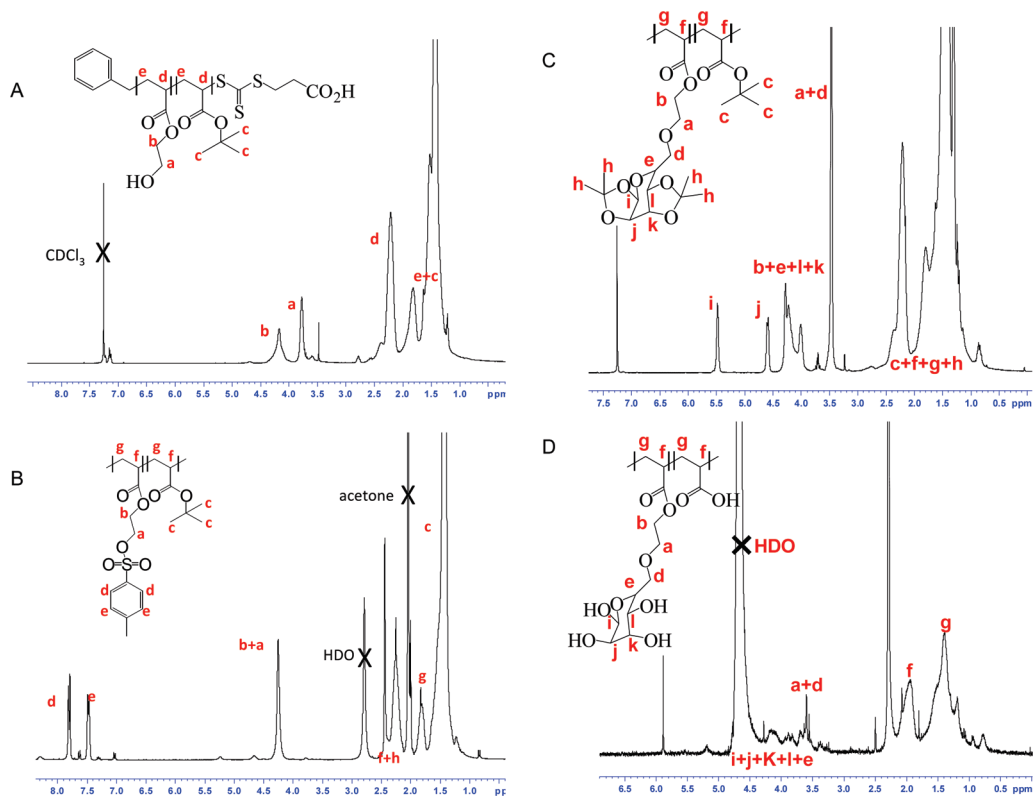
Figure 4. ^{1}H NMR spectra of each step of modification of poly(*tert*-Bu A-*co*-HEA) copolymers: (A) poly(*tert*-Bu A-*co*-HEA) copolymer recorded in CDCl₃; (B) after modification with *p*-toluenesulfonyl chloride recorded in acetone-*d₆*; (C) after modification of 1,2:3,4-di-*O*-isopropylidene-D-galactopyranose in the presence of NaH recorded in CDCl₃; (d) after deprotection of *tert*-butyl groups by TFA treatment to yield poly(AA-*co*-HEA/galactose) recorded in D₂O.

retention times consistent with a chemical modification of the polymer backbone. The presence of a molecular weight shoulder at high retention times is attributed to interchain coupling of the copolymer following the oxidation of thiol into disulfide (Figure S5 in the Supporting Information). After addition of a reducing agent, i.e. DMPP, the shoulder disappears. The polydispersity of the polymer remains relatively narrow (less than 1.3) after modification.

The tertiary ester group (*tert*-butyl group) was then cleaved (vide infra). After purification, the samples were analyzed by FTIR (Figure S6 in the Supporting Information) and ^{1}H NMR (Figure 4) analyses. FTIR spectroscopy confirmed a broad absorption at around 3300 cm^{-1} attributed to carboxylic acid functionality, and an ester absorption band was still observed at 1730 cm^{-1} attributed to the primary ester of HEA. Primary ester bonds are not cleaved by TFA treatment.[86] ^{1}H NMR confirmed that the *tert*-butyl groups were totally cleaved (absence of any signal at 1.4 ppm). The TFA treatment simultaneously cleaved the ketal protection from the galactose to yield free galactose decorated copolymers (the NMR signal assigned to CH of the sugar shifted from 4.8–3.8 ppm to 4.5–3.5 ppm).

3. Layer-by-Layer Assembled of Polymer onto Gold Nanoparticles. The synthesis of gold nanoparticles (reduction of HAuCl₄ by boiling with sodium citrate) yielded spherical gold nanoparticles with highly uniform diameters close to 18 nm as observed by transmission microscopy (TEM) and by dynamic light scattering (DLS) (Figure S7 in the Supporting Information).[77] These reaction conditions can be changed to give GNPs with sizes ranging from 10 to 100 nm.

The sodium citrate plays a double role: first, it induces the reduction of HAuCl₄, and second, it stabilizes the resultant nanoparticles. The presence of sodium citrate on the GNPs prevents their aggregation and precipitation by electrostatic stabilization. The GNP surface charge imparted by the citrate can be further exploited to self-assemble a cationic polymer using electrostatic interactions. In this work, we self-assembled two different polymers in a consecutive LbL process, starting from the anionically charged GNP/citrate surface (see Scheme 1). Successful LbL assembly required a large excess of polymer over gold nanoparticles to avoid the formation of large aggregates, as shown in Figure S8 in the Supporting Information. A similar result was found by Decher et al. for a different system of LbL based on the poly(allylamine hydrochloride) and poly(styrenesulfonate).[17,18]

The multistep self-assembly process was monitored by UV–vis spectrophotometry, DLS, and zeta-potential for each layer. UV–vis revealed an increase in the surface plasmon resonance from 520 to 530 nm with increasing number of layers (Figure S9 in the Supporting Information). The slight increase of the surface plasmon resonance (SPR) wavelength is governed by the mass of polymer present on the GNP surface. The SPR effect arises from the collective oscillation of conduction electrons of the gold upon irradiation with visible light. The characteristic wavelength of maximum absorption and its width depend on the size, shape (spherical presents only one SPR wavelength, while nanorodes present two SPR wavelengths), and dielectric environment of the GNPs. The SPR wavelength exhibits a red shift with any increase in nanoparticle size, along with an overall decrease in the maximum absorbance intensity. A stable, well-dispersed solution of GNPs appears red, as the average interparticle distance is greater than the particle diameter. When particle aggregation occurs, with the average interparticle distance becoming smaller than the particle diameter, the solution turns blue.[87] The SPR effect is also a
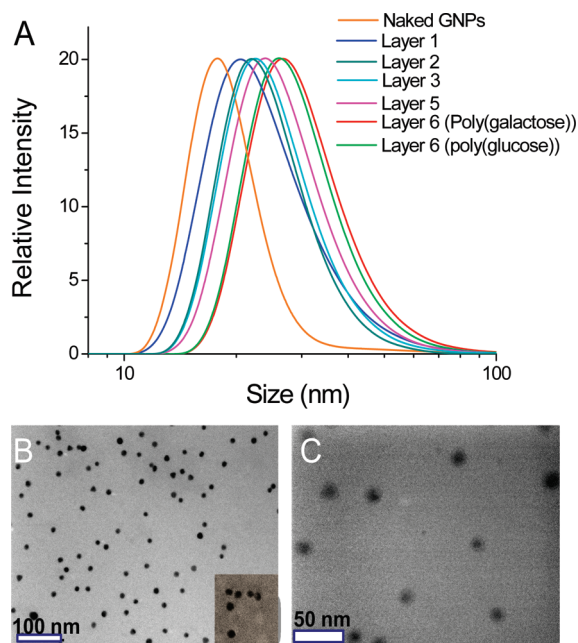
Figure 5. (A) DLS analysis of GNPs modified by different polymer layers. (B) TEM pictures of GNPs after modification by five different layers of polymers and poly(AA-*co*-chloromethylstyrene/glucose). Inset: TEM picture using a negative contrast agent. (C) High magnification of these modified GNPs.

function of the effective refractive index of the metal surface that is determined by the mass of the substances present at the interface and the refractive index of polymers.[88] Consequently in a well-dispersed and stable hybrid GNP solution (i.e., in our case), the changes observed in SPR wavelength (i.e., red shift) is caused by the amount of polymer present at the GNP surface.

DLS results show a slight increase of the nanoparticle diameter size from 18 to 25 ± 5 nm going from naked GNPs to GNPs coated with five layers of polymer. The particle size distribution stays monodisperse and narrow (less than 0.25 determined by DLS), confirming that the nanoparticles are still well-dispersed (Figure 5), congruent with the TEM analyses and UV−vis data.

In the presence of a negative contrast agent (Figure 5B, inset), we observed the presence of a clear halo around the GNPs which we attribute to polymer layers. In addition, Figure 5C shows the TEM pictures of GNPs after modification by five different layers of polymers and poly(AA-*co*-chloromethylstyrene/glucose) at high magnification; we observed the presence of gray halo around of GNPs which we attribute to the polymer shell.

The oscillation of the zeta-potential with each layer deposition is shown in Figure S10 in the Supporting Information, confirming the self-assembly of consecutive layers. Self-limiting assembly, characteristic of the LbL process, was observed by a zeta-potential constant (see Figure S11 in the Supporting Information).

XPS analysis was used to confirm the alternation from cationic to anionic (etc.) charge by the variation of the intensity of the nitrogen signal (around 399 eV) (see Figure 9). The N/C intensity ratio determined by XPS analysis is maximum (around 0.2) when PEI is the outer layer, and minimal (around 0.1) when poly(AA) is the outer layer. According to the position of PEI in the LbL, i.e., inserted between two poly(AA) layers or at the surface of GNPS, i.e., as the last layer, the N(1s) energy bond shifted from 400.0 to 399.0 eV. Between two layers of poly(AA), all
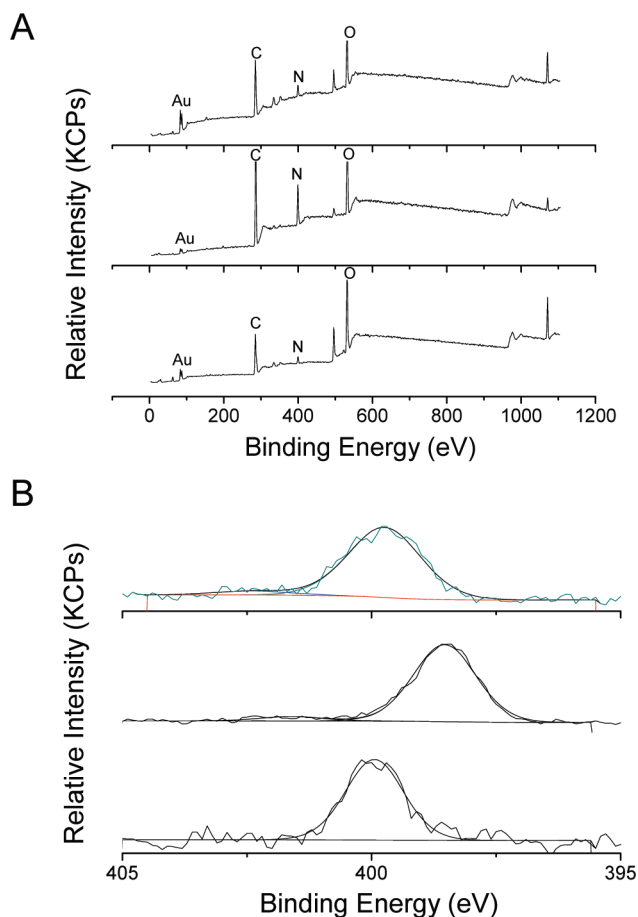

Figure 6. XPS spectra of GNPs at different stages: (A) wide XPS spectra (up) GNPs coated by two layers, i.e. GNPs/PEI/PAA; (middle) GNPs coated by five layers, i.e. GNPs/PEI/PAA/.../PEI; (bottom) GNPs coated by six layers, GNPs/PEI/PAA/.../poly(AA-*co*-galactose). (B) N(1) spectra obtained by XPS analysis: (up) GNPs coated by two layers, i.e. GNPs/PEI/PAA; (middle) GNPs coated by one layer, i.e. GNPs/PEI; (bottom) GNPs coated by six layers, GNPs/PEI/PAA/.../poly(AA-*co*-galactose).

nitrogen atoms of PEI are in quaternized form, resulting in a signal at 400 eV. In the case of PEI being the last layer, the presence of non-quaternized nitrogen can be detected at 399 eV.

Both glycopolymers were introduced to the gold surfaces by the final layer assembly of anionic polymer (the poly(AA-*co*-sugar) copolymers). UV−vis spectroscopy indicated a slight increase in the plasmon resonance wavelength in accord with the addition of the final layer (around 530 nm for both GNPs/glycopolymers). DLS measurements confirmed that the GNPs remained well-dispersed (with a low PDI less than 0.2), with minimal aggregation after modification with the final layer, in accord with TEM analysis (Figure 7). In addition, the zeta-potential showed a significant change of surface charge from $+30.0 \pm 5$ to $\sim-40.0 \pm 5$ mV (Table 2). After coating with the sugar-modified polymer GNPs/poly(AA-*co*-galactose) displayed a zeta-potential around −40.0 mV, while GNPs/poly(AA-*co*-glucose) displayed a zeta-potential around −45.0 mV).

The presence of sugar on the gold surfaces was verified using XPS analysis. C(1s) confirms the presence of ester groups by the characteristic signal at 289.0 eV[89] for poly(AA-*co*-glucose)-modified GNPs (Figure 7). This ester bond is attributed to the HEA monomer units present in the copolymers. In the case of poly(AA-*co*-glucose) obtained by

nucleophilic modification of chloromethylstyrene, S(2p) bond at 162.8 eV was observed. This energy binding is characteristic of −S−C− bonds.[89]

Sugar moieties present a very specific binding affinity to lectins, such as concavalin A. The GNPs/PEI/PAA/.../ P(AA-*co*-sugar) were tested in the presence of a solution of concavalin A to confirm the accessibility of the sugar groups on the nanoparticle surfaces. After exposure to to lectin, the particle size and the plasmon resonance were measured. In the case of GNPs/PEI/.../P(AA-*co*-glucose), we observed a shift in plasmon resonance from 528 to 540 nm (Figure 8); in addition, the peak becomes broader, indicating cross-linking of these nanoparticles due to the multiple interactions of lectin (Con A has four binding sites) with glucose. Figure 8 shows the DLS spectra before and after exposure to Con A. We observed an important shift from 40 nm to ∼1 μm, in accord with changes observed in the Plasmon resonance. After a few hours, the particles totally precipitated in the vials (see Figure 9). However, the glucose/lectin interactions could be easily displaced by the addition of free glucose. We exploited this property to redisperse the nanoparticles. Glucose was added to the solution containing lectin and GNPs (precipitated in the bottom of the tube); after addition of glucose, the nanoparticles were easily redispersed using gentle shaking (Figure 9). DLS and UV−vis confirm that the redispersed GNPs recovered their properties properties, i.e., particle size and plasmon resonance.

After addition of Con A to GNPs/.../P(AA-*co*-galactose), no notable change was observed. The solution stayed well-dispersed for at least 1 day. The absence of change in stability of these particles can be explained by the absence of specific interactions between galactose and Con A, in contrast to interactions with D-mannose and D-glucose.[38,90]

The aggregation, and then the precipitation, of the nanoparticles can be attributed to a loss of stability of the GNPs resulting from nonspecific interactions of Con A with the GNPs surfaces. As a control experiment, we added Con A to a solution of GNPs/.../PAA to confirm that the destabilization resulted from interactions of glucose with Con A.
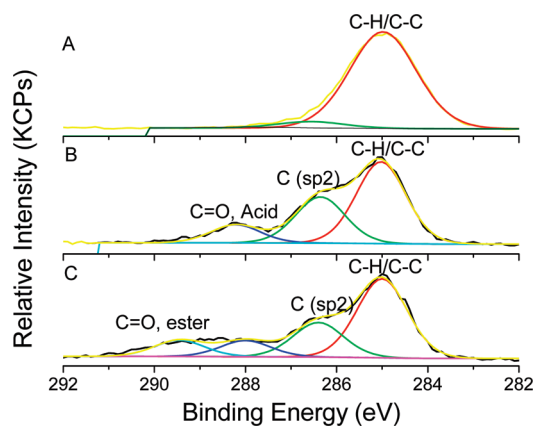
The nanoparticles (with no glucose functionality) remained stable for at least for 1 day, and no changes were noted by DLS and by UV−vis spectrophotometry.
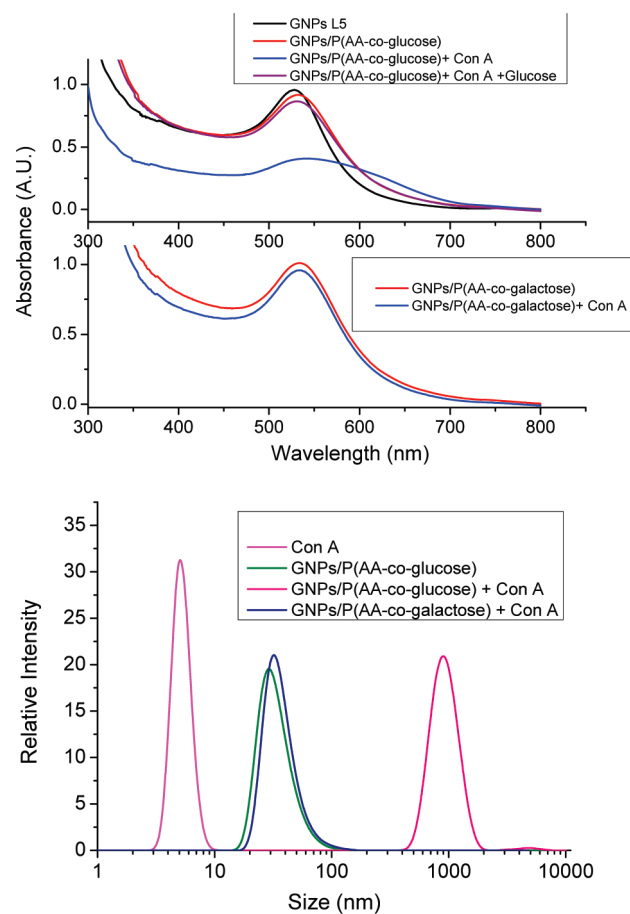

Figure 8. (top) UV−vis and (bottom) DLS spectra of glycopolymer-modified GNPs in the presence of Con A.

Figure 7. C(1s) XPS spectra of GNPs at different stages: (A) GNPs/ PEI; (B) GNPs coated by four layers, i.e. GNPs/PEI/PAA/.../PAA; (C) GNPs coated by six layers, GNPs/PEI/PAA/.../poly(AA-*co*-galactose).
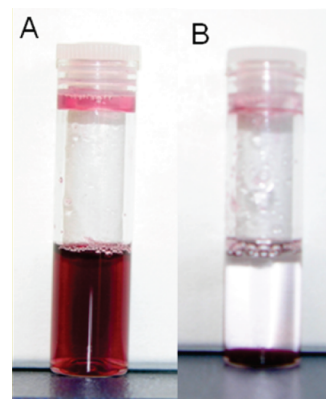

Figure 9. Pictures of (A) GNPs/P(AA-*co*-glucose) in the presence of Con A and after addition of free glucose and (B) before addition of free glucose.

Table 2. Evolution of Zeta-Potential, Surface Plasmon Resonance (SPR), and Dynamic Light Scattering for GNPs Modified with Five Layers of Polymers (GNPs/PEI/.../PEI) and Modified with Glycopolymers (Six Layers)

GNPs	zeta-potential (mV)	SPR (nm)	DLS (nm)
GNPs/PEI/.../PEI	+30.0 ± 5	527	24.0 ± 2
GNPs/PEI/.../P(AA-*co*-glucose)	−45.0 ± 2	528	26.0 ± 2
GNPs/PEI/.../P(AA-*co*-galactose)	−40.0 ± 2	530	27.0 ± 2

Conclusion

Two different methodologies are presented for the attachment of sugar functionality to copolymer chains at quantitative yields. The first approach involves a nucleophilic substitution of chloromethylstyrene using a thiol−sugar (in our case, thioglucose) at room temperature, while the second approach involves modification of the hydroxyl group by a tosylate and then a nucleophilic substitution using a protected galactose. Both of these approaches proved to be relatively simple and efficient. Second, the copolymers were assembled onto gold nanoparticle surfaces using a layer-by-layer methodology. Finally, the nanoparticles modified with P(AA-*co*-glucose) were found to present specific interactions with Con A (lectin).

Supporting Information Available: Kinetic of copolymerization of HEA and *tert*-BuA, GPC traces, characterization of naked GNPs, UV−vis spectra, and zeta-potential for the different LBL are available. This material is available free of charge via the Internet at http://pubs.acs.org.

References and Notes

(1) Boyer, C.; Whittaker, M. R.; Bulmus, V.; Liu, J.; Davis, T. P. *NPG Asia Mater.* **2010**, *2*, 23.

(2) De, M.; Ghosh, P. S.; Rotello, V. M. *Adv. Mater.* **2008**, *20*, 4225.

(3) Ghosh, P. S.; Kim, C.-K.; Han, G.; Forbes, N. S.; Rotello, V. M. *ACS Nano* **2008**, *2*, 2213.

(4) Peer, D.; Karp, J. M.; Hong, S.; Farokhzad, O. C.; Margalit, R.; Langer, R. *Nat. Nanotechnol.* **2007**, *2*, 751.

(5) Alivisatos, A. P. *Nat. Biotechnol.* **2004**, *22*, 47.

(6) Ferrari, M. *Nat. Rev. Cancer* **2005**, *5*, 161.

(7) Guo, C.; Boullanger, P.; Jiang, L.; Liu, T. *Biosens. Bioelectron.* **2007**, *22*, 1830.

(8) Boyer, C.; Bulmus, V.; Priyanto, P.; Teoh, W. Y.; Amal, R.; Davis, T. P. *J. Mater. Chem.* **2009**, *19*, 111.

(9) Boyer, C.; Priyanto, P.; Davis, T. P.; Pissuwan, D.; Bulmus, V.; Kavallaris, M.; Teoh, W. Y.; Amal, R.; Carroll, M.; Woodward, R.; Pierree, T. S. *J. Mater. Chem.* **2010**, *20*, 255.

(10) Gong, X.; Peng, S.; Wen, W.; Sheng, P.; Li, W. *Adv. Funct. Mater.* **2009**, *19*, 292.

(11) Gupta, A. K.; Curtis, A. S. G. *J. Mater. Sci.: Mater. Med.* **2004**, *15*, 493.

(12) Namdeo, M.; Saxena, S.; Tankhiwale, R.; Bajpai, M.; Mohan, Y. M.; Bajpai, S. K. *J. Nanosci. Nanotechnol.* **2008**, *8*, 3247.

(13) Nasongkla, N.; Bey, E.; Ren, J.; Ai, H.; Khemtong, C.; Guthi, J. S.; Shook-Fong Chin, A.; Sherry, D.; Boothman, D. A.; Gao, J. *Nano Lett.* **2006**, *6*, 2427.

(14) Boyer, C.; Whittaker, M.; Luzon, M.; Davis, T. P. *Macromolecules* **2009**, *42*, 6917.

(15) Sumerlin, B. S.; Lowe, A. B.; Stroud, P. A.; Zhang, P.; Urban, M. W.; McCormick, C. L. *Langmuir* **2003**, *19*, 5559.

(16) Lowe, A. B.; Sumerlin, B. S.; Donovan, M. S.; McCormick, C. L. *J. Am. Chem. Soc.* **2002**, *124*, 11562.

(17) Schneider, G.; Decher, G. *Nano Lett.* **2004**, *4*, 1833.

(18) Schneider, G.; Decher, G. *Langmuir* **2008**, *24*, 1778.

(19) Decher, G.; Hong, J. D. *Makromol. Chem., Macromol. Symp.* **1991**, *46*, 321.

(20) Decher, G. *Science* **1997**, *277*, 1232.

(21) Reisch, A.; Hemmerle, J.; Voegel, J.-C.; Gonthier, E.; Decher, G.; Benkirane-Jessel, N.; Chassepot, A.; Mertz, D.; Lavalle, P.; Mesini, P.; Schaaf, P. *J. Mater. Chem.* **2008**, *18*, 4242.

(22) Schneider, G. F.; Decher, G. *Nano Lett.* **2008**, *8*, 3598.

(23) Caruso, F.; Caruso, R. A.; Mohwald, H. *Science* **1998**, *282*, 1111.

(24) Seo, J.; Schattling, P.; Lang, T.; Jochum, F.; Nilles, K.; Theato, P.; Char, K. *Langmuir* **2010**, *26*, 1830.

(25) Dahne, C. S. *Angew. Chem., Int. Ed.* **2004**, *43*, 3762.

(26) Quinn, J. F.; Johnston, A. P. R.; Such, G. K.; Zelikin, A.; Caruso, F. *Chem. Soc. Rev.* **2007**, *36*, 707.

(27) Sexton, A.; Whitney, P. G.; Chong, S.-F.; Zelikin, A. N.; Johnston, A. P. R.; De Rose, R.; Brooks, A. G.; Caruso, F.; Kent, S. J. *ACS Nano* **2009**, *3*, 3391.

(28) Mayya, K. S.; Schoeler, B.; Caruso, F. *Adv. Funct. Mater.* **2003**, *13*, 183.

(29) Gittins, D. I.; Caruso, F. *Adv. Mater.* **2000**, *12*, 1947.

(30) Wang, Y.; Angelatos, A. S.; Caruso, F. *Chem. Mater.* **2008**, *20*, 848.

(31) Kim, J. S.; Rieter, W. J.; Taylor, K. M. L.; An, H.; Lin, W.; Lin, W. *J. Am. Chem. Soc.* **2007**, *129*, 8962.

(32) Chanana, M.; Gliozzi, A.; Diaspro, A.; Chodnevskaja, I.; Huewel, S.; Moskalenko, V.; Ulrichs, K.; Galla, H.-J.; Krol, S. *Nano Lett.* **2005**, *5*, 2605.

(33) Mazumder, M. A. J.; Shen, F.; Burke, N. A. D.; Potter, M. A.; Stver, H. D. H. *Biomacromolecules* **2008**, *9*, 2292.

(34) Wang, S. H.; Shi, X. Y.; Van Antwerp, M.; Cao, Z. Y.; Swanson, S. D.; Bi, X. D.; Baker, J. R. *Adv. Funct. Mater.* **2007**, *17*, 3043–3050.

(35) Elbakry, A.; Zaky, A.; Liebl, R.; Rachel, R.; Goepferich, A.; Breunig, M. *Nano Lett.* **2009**, *9*, 2059.

(36) Schneider, G. F.; Subr, V.; Ulbrich, K.; Decher, G. *Nano Lett.* **2009**, *9*, 636.

(37) Such, G. K.; Tjipto, E.; Postma, A.; Johnston, A. P. R.; Caruso, F. *Nano Lett.* **2007**, *7*, 1706.

(38) Connal, L. A.; Kinname, C. R.; Zelikin, A. N.; Caruso, F. *Chem. Mater.* **2009**, *21*, 576.

(39) Schneider, G.; Decher, G. *Nano Lett.* **2006**, *6*, 530.

(40) Choi, S.-K.; Mammen, M.; Whitesides, G. M. *J. Am. Chem. Soc.* **1997**, *119*, 4103.

(41) Ladmiral, V.; Mantovani, G.; Clarkson, G. J.; Cauet, S.; Irwin, J. L.; Haddleton, D. M. *J. Am. Chem. Soc.* **2006**, *128*, 4823.

(42) Bes, L.; Angot, S.; Limer, A.; Haddleton, D. M. *Macromolecules* **2003**, *36*, 2493.

(43) Haddleton, D. M.; Ohno, K. *Biomacromolecules* **2000**, *1*, 152.

(44) Mammen, M.; Choi, S.-K.; Whitesides, G. M. *Angew. Chem., Int. Ed.* **1998**, *37*, 2754.

(45) Nurmi, L.; Lindqvist, J.; Randev, R.; Syrett, J.; Haddleton, D. M. *Chem. Commun.* **2009**, 2727.

(46) Boyer, C.; Bulmus, V.; Davis, T. P.; Ladmiral, V.; Liu, J.; Perrier, S. *Chem. Rev.* **2009**, *109*, 5402.

(47) McCormick, C. L.; Sumerlin, B. S.; Lokitz, B. S.; Stempka, J. E. *Soft Matter* **2008**, *4*, 1760.

(48) Smitha, A. E.; Xua, X.; McCormick, C. L. *Prog. Polym. Sci.* **2010**, *35*, 45.

(49) Deng, Z.; Ahmed, M.; Narain, R. *J. Polym. Sci., Part A: Polym. Chem.* **2009**, *47*, 614.

(50) Ouchi, M.; Terashima, T.; Sawamoto, M. *Chem. Rev.* **2009**, *109*, 4963.

(51) Rosen, B. M.; Percec, V. *Chem. Rev.* **2009**, *109*, 5069.

(52) Tsarevsky, N. V.; Matyjaszewski, K. *Chem. Rev.* **2007**, *107*, 2270.

(53) Hawker, C. J.; Bosman, A. W.; Harth, E. *Chem. Rev.* **2001**, *101*.

(54) David, G.; Boyer, C.; Tonnar, J.; Ameduri, B.; Lacroix-Desmazes, P.; Boutevin, B. *Chem. Rev.* **2006**, *106*, 3936.

(55) Albertin, L.; Stenzel, M. H.; Barner-Kowollik, C.; Foster, L. J. R.; Davis, T. P. *Macromolecules* **2005**, *38*, 9075.

(56) Zhang, L.; Bernard, J.; Davis, T. P.; Barner-Kowollik, C.; Stenzel, M. H. *Macromol. Rapid Commun.* **2008**, *29*, 123.

(57) Bernard, J.; Hao, X.; Davis, T. P.; Barner-Kowollik, C.; Stenzel, M. H. *Biomacromolecules* **2006**, *7*, 232.

(58) Albertin, L.; Stenzel, M. H.; Barner-Kowollik, C.; Foster, L. J. R.; Davis, T. P. *Macromolecules* **2005**, *38*, 9075.

(59) Albertin, L.; Stenzel, M. H.; Barner-Kowollik, C.; Foster, L. J. R.; Davis, T. P. *Polymer* **2005**, *46*, 2831.

(60) Albertin, L.; Stenzel, M.; Barner-Kowollik, C.; Foster, L. J. R.; Davis, T. P. *Macromolecules* **2004**, *37*, 7530.

(61) Albertin, L.; Kohlert, C.; Stenzel, M.; Foster, L. J. R.; Davis, T. P. *Biomacromolecules* **2004**, *5*, 255.

(62) Bernard, J.; Favier, A.; Zhang, L.; Nilasaroya, A.; Davis, T. P.; Barner-Kowollik, C.; Stenzel, M. H. *Macromolecules* **2005**, *38*, 5475.

(63) Zhang, L.; Nguyen, T. L. U.; Bernard, J.; Davis, T. P.; Barner-Kowollik, C.; Stenzel, M. H. *Biomacromolecules* **2007**, *8*, 2890.

(64) Becer, C. R.; Hoogenboom, R.; Schubert, U. S. *Angew. Chem., Int. Ed.* **2009**, *48*, 4900.

(65) Iha, R. K.; Wooley, K. L.; Nystrom, A. M.; Burke, D. J.; Kade, M. J.; Hawker, C. J. *Chem. Rev.* **2009**, *109*, 5620.

(66) Chen, G.; Amajjahe, S.; Stenzel, M. H. *Chem. Commun.* **2009**, 1198.

(67) Boyer, C.; Bulmus, V.; Davis, T. P. *Macromol. Rapid Commun.* **2009**, *30*, 493.

(68) Witczak, Z. J.; Lorchak, D.; Nguyen, N. *Carbohydr. Res.* **2007**, *342*, 1929.

(69) Ott, C.; Hoogenboom, R.; Schubert, U. S. *Chem. Commun.* **2008**, 3516.

(70) Becer, C. R.; Babiuch, K.; Pilz, D.; Hornig, S.; Heinze, T.; Gottschaldt, M.; Schubert, U. S. *Macromolecules* **2009**, *42*, 2387.

(71) Boyer, C.; Davis, T. P. *Chem. Commun.* **2009**, *40*, 6029.

(72) Gibson, M. I.; Froehlich, E.; Klok, H.-A. *J. Polym. Sci., Part A: Polym. Chem.* **2009**, *47*, 4332.

(73) Housni, A.; Cai, H.; Liu, S.; Pun, S. H.; Narain, R. *Langmuir* **2007**, *23*, 5056.

(74) Narain, R.; Housni, A.; Gody, G.; Boullanger, P.; Charreyre, M.-T.; Delair, T. *Langmuir* **2007**, *23*, 12835.

(75) Deng, Z.; Li, S.; Jiang, X.; Narain, R. *Macromolecules* **2009**, *42*, 6393.

(76) Stenzel, M. H.; Davis, T. P. *J. Polym. Sci., Part A: Polym. Chem.* **2002**, *40*, 4498.

(77) Frens, G. *Nat. Phys. Sci.* **1973**, *241*, 20.

(78) Rosen, B. M.; Lligadas, G.; Hahn, C.; Percec, V. *J. Polym. Sci., Part A: Polym. Chem.* **2009**, *47*, 3931.

(79) Xu, J.; Tao, L.; Boyer, C.; Lowe, A. B.; Davis, T. P. *Macromolecules* **2010**, *43*, 20.

(80) Harrisson, S. *Macromolecules* **2009**, *42*, 897.

(81) Boyer, C.; Liu, J.; Bulmus, V.; Davis, T. P. *Aust. J. Chem.* **2009**, *62*, 830.

(82) York, A. W.; Scales, C. W.; Huang, F.; McCormick, C. L. *Biomacromolecules* **2007**, *8*, 2337.

(83) Boyer, C.; Granville, A.; Davis, T. P.; Bulmus, V. *J. Polym. Sci., Part A: Polym. Chem.* **2009**, *47*, 3773.

(84) Ellman, G. L. *Arch. Biochem. Biophys.* **1958**, *74*, 443.

(85) Ellman, G. L. *Arch. Biochem. Biophys.* **1959**, *82*, 70.

(86) Boyer, C.; Boutevin, G.; Robin, J.-J.; Boutevin, B. *J. Polym. Sci., Part A: Polym. Chem.* **2007**, *45*, 395.

(87) Elghanian, R.; Storhoff, J. J.; Mucic, R. C.; Letsinger, R. L.; Mirkin, C. A. *Science* **1997**, *277*, 1078.

(88) Sota, H.; Hasegawa, Y.; Iwakura, M. *Anal. Chem.* **1998**, *70*, 2019.

(89) Beamson, G.; Briggs, D. *High Resolution XPS of Organic Polymers the Scienta ESCA300 Database*; Wiley: New York, 1992.

(90) Cairo, C. W.; Gestwicki, J. E.; Kanai, M.; Kiessling, L. L. *J. Am. Chem. Soc.* **2002**, *124*, 1615.